X-ray Absorption Edge Determination of the Oxidation State and Coordination Number of Copper: Application to the Type 3 Site in *Rhus vernicifera* Laccase and Its Reaction with Oxygen

Lung-Shan Kau, Darlene J. Spira-Solomon, James E. Penner-Hahn, Keith O. Hodgson,* and Edward I. Solomon*

Contribution from the Department of Chemistry, Stanford University, Stanford, California 94305. *Received November 19, 1986*

Abstract: Cu X-ray absorption edge features of 19 Cu(I) and 40 Cu(II) model complexes have been systematically studied and correlated with oxidation state and geometry. Studies of Cu(I) model complexes with different coordination number reveal that an 8983–8984-eV peak (assigned as the Cu 1s → 4p transition) can be correlated in energy, shape, and intensity with ligation and site geometry of the cuprous ion. These Cu(I) edge features have been qualitatively interpreted with ligand field concepts. Alternatively, no Cu(II) complex exhibits a peak below 8985.0 eV. The limited intensity observed in the 8983–8985-eV region for some Cu(II) complexes is associated with the tail of an absorption peak at ~8986 eV which is affected by the covalency of the equatorial ligands. These model studies allow accurate calibration of a normalized difference edge procedure which is used for the quantitative determination of Cu(I) content in copper complexes of mixed oxidation state composition. This normalized difference edge analysis is then used to quantitatively determine the oxidation states of the copper sites in type 2 copper-depleted (T2D) and native forms of the multicopper oxidase, *Rhus vernicifera* laccase. The type 3 site of the T2D laccase is found to be fully reduced and stable to oxidation by O_2 or by 25-fold protein equivalents of ferricyanide, but it can be oxidized by reaction with peroxide. The increase in intensity of the 330-nm absorption feature which results from peroxide titration of T2D laccase is found to correlate linearly with the percent of oxidation of the binuclear copper site. This correlation indicates that peroxide oxidizes but does not bind to the T3 site. We have used this correlation to determine that native laccase, as isolated, contains 22 ± 3% reduced T3 sites and that all spectral changes observed upon peroxide addition to native laccase can be accounted for by oxidation of these reduced sites. In the presence of azide and peroxide, further reduction occurs and as much as 40% of the binuclear copper pairs are stabilized in the reduced state. The importance of these results to previous reports of peroxide binding at the laccase active site is discussed.

The active sites of a number of metalloproteins (including hemocyanin, tyrosinase, laccase, ceruloplasmin, and ascorbic acid oxidase) contain a coupled binuclear copper site which, when in its cuprous oxidation state, reacts with dioxygen.[1] For all of these enzymes, it is important to define the geometric and electronic structure of the reduced site and further to clearly determine the oxidation state of the coppers upon reaction with dioxygen and the two-electron reduced peroxide molecule. As presented in the previous paper,[2] determination of the oxidation state of the coupled binuclear copper site in laccase[3] and its type 2 copper-depleted (T2D) derivative[4] has become a particularly important problem with respect to defining its mechanism in catalyzing the four-electron reduction of dioxygen to water. In the reduced state, the two Cu(I)'s are in a d^{10} closed shell electronic configuration and thus their geometric and electronic structure cannot be probed by EPR and optical methods. Further, when oxidized, the two cupric ions are antiferromagnetically coupled through an endogenous bridging ligand, resulting in no EPR signal; in the absorption spectrum, only broad, near-UV intensity at ≤350 nm has been associated[2,5] with the coupled binuclear cupric site. Thus, determination of the oxidation state of these coupled sites is not accessible by conventional spectral methods. In this study, we have developed the utility of X-ray absorption edge spectroscopy as a *direct* probe of the oxidation state and of the geometric and electronic structure of copper sites in proteins. We have then applied this technique to clearly define the oxidation state of the coupled binuclear copper site in important forms of laccase.

Rhus vernicifera laccase is a multicopper oxidase[3] that contains in addition to a coupled binuclear copper center (called type 3) a blue (type 1) and a normal (type 2) center for a total of four copper ions at its active site. In laccase, the oxidized type 3 site is a two-electron acceptor and displays a broad near-UV feature maximizing at 330 nm, $\epsilon = 2800\ M^{-1}\ cm^{-1}$.[5] Upon reaction with peroxide,[6] an additional $\Delta\epsilon = 800\ M^{-1}\ cm^{-1}$ is observed at ~330 nm; azide reaction results in significant $N_3^- \rightarrow$ Cu(II) charge-transfer (CT) intensity in the 550–340-nm region.[7] The type 2 copper can be selectively removed[4] from native laccase to generate the T2D protein form which, in contrast to native laccase, exhibits no near-UV absorption feature in the 330-nm region[8] and no $N_3^- \rightarrow$ Cu(II) CT transition when reacted with azide.[8] However, peroxide addition to T2D results in a new absorption feature at 330 nm ($\Delta\epsilon \sim 2000\ M^{-1}\ cm^{-1}$), and this form does display $N_3^- \rightarrow$ Cu(II) CT intensity ($\Delta\epsilon_{450} = 900\ M^{-1}\ cm^{-1}$), suggesting that the type 3 site is reduced in the original T2D and oxidized by H_2O_2.[9] In contrast to this apparent reduction of the type 3 site, other studies report that T2D does display absorption intensity in the 330-nm region[10] and accepts three reducing equivalents in reductive titration studies,[10,11] suggesting that the type 3 site is

(1) Solomon, E. I. In *Copper Proteins*; Spiro, T. G., Ed.; Wiley-Interscience: New York, 1981.
(2) Spira-Solomon, D. J.; Solomon, E. I. *J. Am. Chem. Soc.*, preceding paper in this issue.
(3) (a) Fee, J. A. *Struct. Bonding (Berlin)* **1975**, *23*, 1–60. (b) Malkin, R.; Malmstrom, B. G. *Adv. Enzymol.* **1970**, *33*, 177–244.
(4) Graziani, M. T.; Morpurgo, L.; Rotilio, G.; Mondovi, B. *FEBS Lett.* **1976**, *70*, 87–90.
(5) Reinhammar, B. *Biochim. Biophys. Acta* **1972**, *275*, 245–259.
(6) (a) Farver, O.; Goldberg, M.; Lancet, D.; Pecht, I. *Biochem. Biophys. Res. Commun.* **1976**, *73*, 494–500. (b) Farver, O.; Goldberg, M.; Pecht, I. *FEBS Lett.* **1978**, *94*, 383–386. (c) Farver, O.; Goldberg, M.; Pecht, I. *Eur. J. Biochem.* **1980**, *104*, 71–77.
(7) (a) Morpurgo, L.; Rotilio, G.; Finazzi-Agro, A.; Mondovi, B. *Biochim. Biophys. Acta* **1974**, *336*, 324–328. (b) Winkler, M. E.; Spira, D. J.; LuBien, C. D.; Thamann, T. J.; Solomon, E. I. *Biochem. Biophys. Res. Commun.* **1982**, *107*, 727–734.
(8) (a) Morpurgo, L.; Graziani, M. T.; Finazzi-Agro, A.; Rotilio, G.; Mondovi, B. *Biochem. J.* **1980**, *187*, 361–366. (b) Morpurgo, L.; Graziani, M. T.; Desideri, A.; Rotilio, G. *Biochem. J.* **1980**, *187*, 367–370.
(9) LuBien, C. D.; Winkler, M. E.; Thamann, T. J.; Scott, R. A.; Co, M. S.; Hodgson, K. O.; Solomon, E. I. *J. Am. Chem. Soc.* **1981**, *103*, 7014–7016.
(10) (a) Reinhammar, B.; Oda, Y. *J. Inorg. Biochem.* **1979**, *11*, 115–127. (b) Reinhammar, B. *J. Inorg. Biochem.* **1983**, *18*, 113–121.

0002-7863/87/1509-6433$01.50/0

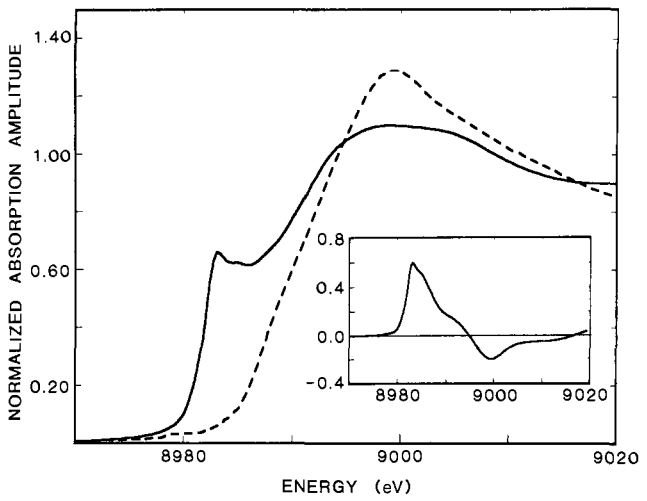

Figure 1. Typical Cu(I) (I-10, —) and Cu(II) (II-20, ---) X-ray absorption edge spectra, normalized as described in the Experimental Section. (See Table II for structures of these two compounds.) Inset: Normalized difference edge spectrum for I-10 minus II-20.

oxidized. All of these absorption studies, however, only indirectly probe the copper ion oxidation state.

X-ray absorption spectroscopy is a direct method that can probe the electronic and structural nature of the metal site.[12] Empirical correlations of the energies of copper X-ray absorption edge features have been used to detect the presence of Cu(I). It has long been recognized that the pre-edge feature at 8984 eV is present in the absorption edge spectra of Cu(I) complexes but not in those of Cu(II), as shown in Figure 1. Chan et al. further used the intensity of the 8984-eV feature for properly normalized spectra to show that one of the two copper ions in resting oxidized cytochrome *c* oxidase is reduced.[13] However, it has been reported[14] that covalent Cu(II) can also contribute intensity in this 8984-eV region. The 8984-eV pre-edge feature of Cu(I) complexes has been assigned empirically as a Cu 1s → 4s transition[13-16] or alternatively as a Cu 1s → 4p transition from polarized single-crystal studies.[17] In the X-ray absorption edge spectra of Cu(II) complexes, the first intense transition occurs at 8986 eV; a very weak feature is observed at lower energy (8979 eV) which has been proposed[18] as the 1s → 3d transition and confirmed by single-crystal studies.[19] The assignment of the Cu(II) 8986-eV feature remains controversial and could be either 1s → 4s,[20] 1s → 4p,[21] or 1s → 4p simultaneous with a ligand-to-metal shake-down transition.[22]

Our earlier studies,[9] using X-ray absorption edge comparisons of T2D laccase samples with Cu(I) and Cu(II) imidazole solutions, qualitatively demonstrated by the presence of a significant peak at 8984 eV that T2D laccase contains a binuclear cuprous type 3 site which was stable with respect to oxidation by dioxygen but could be oxidized by H_2O_2; analogous oxidation reactions of the type 3 site were found to occur for the native enzyme.[23] In order to quantitatively estimate the amount of Cu(I) present in these different forms of laccase, we have developed a difference edge analysis procedure[23] that involves normalization of the edge spectrum of a protein sample containing an unknown amount of Cu(I) followed by subtraction of the normalized edge of the fully oxidized Cu(II) form of the protein. This subtraction results in a derivative-shaped peak (Figure 1, inset) where the peak height of the positive component at 8984 eV reflects the amount of Cu(I) present. The derivative shape results from the fact that with proper normalization a Cu(II) sample has significantly higher peak amplitude at 9000 eV relative to Cu(I), producing the negative feature at higher energy.

The error involved in the quantitation of Cu(I) content by this normalized difference edge analysis method critically depends on understanding the variability in the pre-edge features of copper model compounds. We report herein the systematic X-ray absorption edge studies of a wide range of Cu(I) and Cu(II) model compounds having different coordination numbers, geometries, and degrees of covalency. We further interpret the Cu(I) pre-edge features (energy position, edge shape, and amplitude) in terms of ligand field concepts. From a detailed understanding of Cu(I) edge features, we can estimate the coordination number of the reduced type 3 copper site and from accurate calibration of the normalized difference edges we can quantitatively determine the reduced copper content in T2D laccase. Having quantitated the difference edge of a reduced type 3 site through model studies, we then use the normalized difference edge of the reduced minus oxidized binuclear type 3 site in T2D to investigate the extent of oxidation of this binuclear site in reactions of T2D and native laccase with dioxygen and peroxide.

Experimental Section

Native laccase was purified[24] from the acetone powder (Saito and Co., Osaka, Japan) of the Japanese lacquer tree, *Rhus vernicifera*, to a purity ratio A_{280}/A_{614} = 15.0–16.5, as modified in the previous article.[2] T2D laccase was prepared following the procedure of Graziani et al.[4]

Water was purified to a resistivity of 15–18 MΩ cm via a Sybron Barnstead Nanopure deionizing system. All studies utilized reagent grade chemicals without further purification in 0.1 M potassium phosphate, pH 6.0. A 30% solution of hydrogen peroxide was standardized by permanganate.[25] Protein samples were concentrated to ~1 mM by Amicon ultrafiltration (Amicon Corp., MA) through PM-10 or YM-10 membranes.

Optical absorption spectra were measured at room temperature on a Cary 14 spectrophotometer. A Bruker ER 220-D-SRC EPR spectrometer (operating at 10 mW microwave power, 20 G modulation amplitude, and a frequency of 9.27 GHz) was used to examine frozen protein solutions at 77 K in a finger dewar. For each sample to be examined by X-ray absorption edge spectroscopy, the characterization procedure consisted of recording the 298 K UV–vis absorption spectrum of the concentrated protein sample in a 1-mm quartz cell, transferring the protein into the X-ray cell, freezing the cell in liquid N_2, recording its EPR spectrum, transporting the frozen sample to the Stanford Synchrotron Radiation Laboratory (SSRL) for recording the XAS spectra,

(11) (a) Farver, O.; Frank, P.; Pecht, I. *Biochem. Biophys. Res. Commun.* **1982**, *108*, 273–278. (b) Frank, P.; Farver, O.; Pecht, I. *J. Biol. Chem.* **1983**, *258*, 11112–11117. (c) Frank, P.; Pecht, I. *Biochem. Biophys. Res. Commun.* **1983**, *114*, 57–64. (d) Frank, P.; Farver, O.; Pecht, I. *Inorg. Chim. Acta* **1984**, *91*, 81–88.

(12) (a) Cramer, S. P.; Hodgson, K. O. *Prog. Inorg. Chem.* **1979**, *25*, 1–39. (b) Lee, P. A.; Citrin, P. H.; Eisenberger, P.; Kincaid, B. M. *Rev. Mod. Phys.* **1981**, *53*, 769–806. (c) Solomon, E. I. In *Comments of Inorganic Chemistry*; Sutin, Norman, Ed.; Gordon & Breach: New York, 1984; Vol. 3, pp 225–320.

(13) Hu, V. W.; Chan, S. I.; Brown, G. S. *Proc. Natl. Acad. Sci. U.S.A.* **1977**, *74*, 3821–3825.

(14) Powers, L.; Blumberg, W. E.; Chance, B.; Barlow, C.; Leight, J. S., Jr.; Smith, J. C.; Yonetani, T.; Vik, S.; Peisach, J. *Biochim. Biophys. Acta* **1979**, *546*, 520–538.

(15) Blumberg, W. E.; Peisach, J.; Eisenberger, P.; Fee, J. A. *Biochemistry* **1978**, *17*, 1842–1846.

(16) Brown, J. M.; Powers, L.; Kincaid, B.; Larrabee, J. A.; Spiro, T. G. *J. Am. Chem. Soc.* **1980**, *102*, 4210–4216.

(17) Smith, T. A.; Penner-Hahn, J. E.; Hodgson, K. O.; Berding, M. A.; Doniach, S. *Springer Proc. Phys.* **1984**, *2*, 58–60.

(18) Shulman, R. G.; Yafet, T.; Eisenberger, P.; Blumberg, W. E. *Proc. Natl. Acad. Sci. U.S.A.* **1976**, *73*, 1384–1388.

(19) Hahn, J. E.; Scott, R. A.; Hodgson, K. O.; Doniach, S.; Desjardins, S. E.; Solomon, E. I. *Chem. Phys. Lett.* **1982**, *88*, 595–598.

(20) (a) Srivastava, U. C.; Nigam, H. L. *Coord. Chem. Rev.* **1973**, *9*, 275–310 and references therein. (b) Agarwal, B. K.; Bhargava, C. B.; Vishnoi, A. N.; Seth, V. P. *J. Phys. Chem. Solids* **1976**, *37*, 725–728. (c) Kostroun, V. O.; Fairchild, C. A.; Kukkonen, C. A.; Wilkins, J. W. *Phys. Rev. B* **1976**, *13*, 3268–3271. (d) Rao, B. J.; Chetal, A. R. *J. Phys. C: Solid State Phys.* **1982**, *15*, 6281–6284.

(21) Smith, T. A.; Berding, M.; Penner-Hahn, J. E.; Doniach, S.; Hodgson, K. O. *J. Am. Chem. Soc.* **1985**, *107*, 5945–5955.

(22) (a) Blair, R. A.; Goddard, W. A. *Phys. Rev. B* **1980**, *22*, 2767–2776. (b) Kosugi, N.; Yokoyama, T.; Asakuna, K.; Kuroda, H. *Springer Proc. Phys.* **1984**, *2*, 55–57. (c) Kosugi, N.; Yokoyama, T.; Asakuna, K.; Kuroda, H. *Chem. Phys.* **1984**, *91*, 249–256.

(23) (a) Hahn, J. E.; Co, M. S.; Spira, D. J.; Hodgson, K. O.; Solomon, E. I. *Biochem. Biophys. Res. Commun.* **1983**, *112*, 737–745. (b) Penner-Hahn, J. E.; Hedman, B.; Hodgson, K. O.; Spira, D. J.; Solomon, E. I. *Biochem. Biophys. Res. Commun.* **1984**, *119*, 567–575.

(24) Reinhammar, B. *Biochim. Biophys. Acta* **1970**, *205*, 35–47.

(25) Kolthoff, I. M.; Sandell, E. B.; Meehan, E. J.; Bruckenstein, S. *Quantitative Chemical Analysis*; Macmillan: New York, 1969.

re-recording the EPR spectrum of the sample after irradiation, and then thawing the sample for UV–vis characterization in the 1-mm cell. Atomic absorption analysis for total copper present was routinely performed with a Perkin-Elmer 2380 spectrophotometer equipped with a HGA-400 graphite furnace. A copper standard solution was diluted in the protein buffer matrix for each run, monitoring absorption at 324.7 nm with a slit width of 0.7 nm.

XAS protein sample cells were constructed from lucite (outer dimensions 2 × 4 × 25 mm, volume 180 μL) with an X-ray transparent (50 μm Mylar, 25 μm acetate adhesive) front surface and could be used for X-ray fluorescence and EPR measurements. All X-ray absorption data were measured at SSRL on a variety of beam lines between 1983 and 1985. Both parasitic and dedicated running conditions were utilized; the only effect that this had on the data was an increase in the measurement time required during parasitic conditions. Energy monochromatization was accomplished by using a double crystal monochromator containing either Si(111) or Si(220) crystals. Data for protein samples were measured under both focused and unfocused conditions and recorded as fluorescence excitation spectra utilizing either an array of 8–20 NaI(Tl) detectors[26] or a single ionization chamber[27] as the fluorescence detector. Between 4 and 21 15-min scans were measured for each protein sample and then averaged to give the reported spectra. Alternatively, data of copper model compounds were measured only under unfocused conditions and recorded in the transmission mode.

A Cu foil internal energy calibration was measured simultaneously with each protein spectrum.[28] The energy was defined by assigning the first inflection point of the Cu foil spectrum to 8980.3 eV. This method allows determination of relative energies to within 0.2 eV for samples measured under similar conditions and about 1.0 eV for samples measured under different conditions. In all of the work reported below, differences are calculated only between samples measured under similar conditions; thus, energy calibration will not affect the amplitude calculations.

One significant variable between different experimental conditions is the energy resolution of the incident beam which is affected by the monochromator crystals and by the presence or absence of a focusing mirror. The best resolution was for an unfocused beam line with Si(220) crystals, followed by an unfocused beam line with Si(111) crystals, and the lowest resolution is from a focused beam line with Si(220) crystals.

If areas rather than peak heights were used in the edge quantitation, differences in resolution would not be important. However, we have found that it is extremely difficult to remove the absorption edge background accurately, since the background is strongly affected by structure-sensitive continuum resonance transitions. Since the peak height at 8984 eV is less affected by background, we have found heights to be a better measure of Cu(I) content than are areas.

While the model compounds were run under the highest resolution conditions, the data of protein samples were obtained with different resolutions. In order to compare these results, the protein data were all adjusted to the same resolution. In principle, it is possible to deconvolve the low-resolution data by using the appropriate energy-broadening function.[29] In practice, this is a numerically unstable procedure and requires precise knowledge of the energy-broadening function. Since this function depends on the details of the mirror position and the synchrotron operating parameters and is in general not known, we have adopted the simpler procedure of broadening the high-resolution data.

As a broadening function we have utilized rectangular, triangular, Lorentzian, and Gaussian functions. The procedure is to convolve the highest resolution Cu foil data with each function and to iteratively adjust the width of the broadening function to give numerically the best least-squares agreement between the convolved Cu foil and an authentic lower resolution Cu foil measured simultaneously with the sample. The convolution was performed via numerical integration of the product of the X-ray absorption edge data and the appropriate broadening function. This empirical broadening function is then convolved with the high-resolution protein data to give the equivalent low-resolution protein spectrum. The quantitative difference calculations gave identical results independent of which type of broadening function was used, hence we are confident that this procedure permits accurate comparisons of different resolution data. The broadening functions necessary to compare these data and their effects on the calculated difference spectra are summarized in Table I.

For the difference edge analysis, we have adopted a procedure similar to that of Chan and co-workers,[13,30] in which one measures the absorption well above the edge (into the EXAFS region) and extrapolates this absorption back to the edge energy by fitting a smooth first-order polynomial (to 9000 eV for Cu). In a similar manner, using a smooth polynomial (first or second order depending on data), the pre-edge absorption is extrapolated forward to the edge energy and the normalization is adjusted to give a unit difference, at 9000 eV, between these extrapolations.

Table I. Broadening Functions and Their Effect on Difference Amplitudes

	high resolution[a]		intermediate resolution[a]	
	width[c]	reduction factor[d]	width[c]	reduction factor[d]
rectangle	0.9 ± 0.1	0.84	0.7 ± 0.1	0.89
triangle	1.9 ± 0.2	0.84	1.6 ± 0.2	0.89
Gaussian	3.2 ± 0.3	0.84	2.7 ± 0.3	0.89
Lorentzian	2.3 ± 0.2	0.84	1.9 ± 0.2	0.89

[a] Unfocused, Si(220) monochromator crystals. [b] Unfocused, Si(111) monochromator crystals. [c] Width of convolving function necessary to broaden the data to the equivalent of low resolution (focused, Si(220) monochromator crystals). Width defined as half-width at half-maximum for rectangle and Lorentzian, full-width at half-maximum for triangle, and half-width at 1/e of maximum for Gaussian. [d] Ratio of difference amplitude calculated at the energy which gives maximum difference amplitude (typically at 8984 eV), for broadened data divided by un-broadened data. Note that the ratio is independent of the broadening function used.

Results and Analysis

(A) Model Compound Studies. X-ray absorption K edges have been measured for 19 Cu(I) and 40 Cu(II) complexes which are listed in Table II (I = Cu(I), II = Cu(II)). The Cu(I) complexes

(26) Cramer, S. P.; Scott, R. A. *Rev. Sci. Instrum.* **1981**, *52*, 395–399.
(27) Stern, E. A.; Heald, S. M. *Rev. Sci. Instrum.* **1979**, *50*, 1579–1582.
(28) Scott, R. A.; Hahn, J. E.; Doniach, S.; Freeman, H. C.; Hodgson, K. O. *J. Am. Chem. Soc.* **1982**, *104*, 5364–5369.
(29) Glatter, O. *J. Appl. Crystallogr.* **1974**, *7*, 147–153.

(30) Hu, V. W.; Chan, S. I.; Brown, G. S. *FEBS Lett.* **1977**, *84*, 287–290.
(31) (a) Sorrell, T. N.; Jameson, D. L. *J. Am. Chem. Soc.* **1982**, *104*, 2053–2054. (b) Hendriks, H. M. J.; Birker, P. J. M. W. L.; van Rijn, J.; Verschoor, G. C.; Reedijk, J. *J. Am. Chem. Soc.* **1982**, *104*, 3607–3617. (c) Sorrell, T. N.; Jameson, D. L. *J. Am. Chem. Soc.* **1983**, *105*, 6013–6018. (d) See ref 34. (e) Ormont, B. P. *Structure of Inorganic Substances*; Gostekhizdat: Moscow, 1950. (f) See ref 35. (g) Dagdigian, J. V.; McKee, V.; Reed, C. A. *Inorg. Chem.* **1982**, *21*, 1332–1342. (h) Gagne, R. R.; Kreh, R. P.; Dodge, J. A. *J. Am. Chem. Soc.* **1979**, *101*, 6917–6927. (i) Sorrell, T. N.; Malachowski, M. R.; Jameson, D. L. *Inorg. Chem.* **1982**, *21*, 3250–3252. (j) Weininger, M. S.; Hunt, G. W.; Amma, E. L. *J. Chem. Soc., Chem. Commun.* **1972**, 1140–1141. (k) Coucouvanis, D.; Murphy, C. N.; Kanodia, S. K. *Inorg. Chem.* **1980**, *19*, 2993–2998. (l) Dance, I. G.; Calabrese, J. C. *Inorg. Chim. Acta* **1976**, *19*, L41–L42. (m) Nilsson, K.; Oskarsson, A. *Acta Chem. Scand.* **1982**, *A36*, 605–610. (n) Karlin, K. D.; Hayes, J. C.; Hutchinson, J. P.; Hyde, J. R.; Zubieta, J. *Inorg. Chim. Acta* **1982**, *64*, L219–L220. (o) See ref 46a. (p) Olmstead, M. M.; Musker, W. K.; Kessler, R. M. *Inorg. Chem.* **1981**, *20*, 151–157. (q) Ivarsson, G. *Acta Chem. Scand.* **1973**, *27*, 3523–3530. (r) Fransson, G.; Lundberg, B. K. S. *Acta Chem. Scand.* **1972**, *26*, 3969–3976. (s) McFadden, D. L.; McPhail, A. T.; Garner, C. D.; Mabbs, F. E. *J. Chem. Soc., Dalton Trans.* **1976**, 47–52. (t) Morosin, B. *Acta Crystallogr.* **1969**, *B25*, 19–30. (u) Galy, J.; Jaud, J.; Kahn, O.; Tola, P. *Inorg. Chim. Acta* **1979**, *36*, 229–236. (v) Okawa, H.; Kanda, W.; Kida, S. *Chem. Lett. (Jpn.)* **1980**, 1281–1284. (w) O'Connor, C. J.; Freybery, D. P.; Sinn, E. *Inorg. Chem.* **1979**, *18*, 1077–1088. (x) Countryman, R. M.; Robinson, W. T.; Sinn, E. *Inorg. Chem.* **1974**, *13*, 2013–2020. (y) Mastropaolo, D.; Powers, D. A.; Potenza, J. A.; Schugar, H. J. *Inorg. Chem.* **1976**, *15*, 1444–1449. (z) Freeman, H. C.; Szymanski, J. T. *Acta Crystallogr.* **1967**, *22*, 406–417. (aa) Bacon, G. E.; Curry, N. A. *Proc. R. Soc. London* **1962**, *A266*, 95–108. (bb) Starikova, Z. A.; Shugam, E. A. *Zhur. Strukt. Khim.* **1969**, *10*, 290–293. (cc) Barclay, G. A.; Kennard, C. H. L. *J. Chem. Soc.* **1961**, 3289–3294. (dd) Brown, G. M.; Chidanbaram, *R. Acta Crystallogr.* **1973**, *B29*, 2393–2403. (ee) Simonov, Y. A.; Malinovskii *Sov. Phys. Crystallogr. (Engl. Transl.)* **1970**, *15*, 310–311. (ff) O'Connor, B. H.; Maslen, E. N. *Acta Crystallogr.* **1966**, *20*, 824–835. (gg) Asbrink, S.; Norrby, L.-J. *Acta Crystallogr.* **1970**, *B26*, 8–15. (hh) McKee, V.; Dagdigian, J. V.; Bau, R.; Reed, C. A. *J. Am. Chem. Soc.* **1981**, *103*, 7000–7001. (ii) Dagdigian, J. V.; McKee, V.; Reed, C. A. *Inorg. Chem.* **1982**, *21*, 1332–1342. (jj) McKee, V.; Zvagulis, M.; Reed, C. A. *Inorg. Chem.* **1985**, *24*, 2914–2919. (kk) Coughlin, P. K.; Lippard, S. J. *J. Am. Chem. Soc.* **1981**, *103*, 3228–3229. (ll) Kolks, G.; Lippard, S. J. *Acta Crystallogr.* **1984**, *C40*, 261–271. (mm) Udupa, M. R.; Krebs, B. *Inorg. Chim. Acta* **1979**, *33*, 241–244. (nn) McGinnety, J. A. *J. Am. Chem. Soc.* **1972**, *94*, 8406–8413. (oo) Lee, C.-W.; Anson, F. C. *Inorg. Chem.* **1984**, *23*, 837–844. (pp) Addison, A. W.; Sinn, E. *Inorg. Chem.* **1983**, *22*, 1225–1228. (qq) Glick, M. D.; Gavel, D. P.; Diaddario, L. L.; Rorabacher, D. B. *Inorg. Chem.* **1976**, *15*, 1190–1193. (rr) O'Connor, B. H.; Maslen, E. N. *Acta Crystallogr.* **1966**, *21*, 828–830. (ss) Blumberg, W. E.; Peisach, J. *J. Chem. Phys.* **1968**, *49*, 1793–1802. (tt) Eccles, T. K. Ph.D. Thesis, Stanford University, 1978.

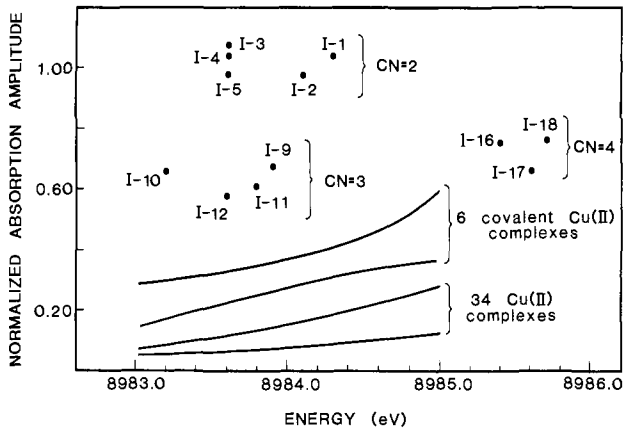

Figure 2. Summary of representative amplitudes of normalized edge spectra for Cu(I) and Cu(II) complexes between 8983.0 and 8986.0 eV. Amplitudes of pre-edge features for Cu(I) complexes are indicated by points. Two amplitude–energy ranges covered by the low energy absorption tails of Cu(II) complexes are indicated: one for 34 normal Cu(II) complexes, the second for 6 covalent Cu(II) complexes (see Results, section A2).

studied have systematic variations in coordination number, geometry, and degree of covalency, while the Cu(II) complexes have an approximately tetragonal geometry but with variations in type of ligands and degree of covalency. These spectra have all been subjected to accurate energy calibration and have been carefully normalized as described in the Experimental Section. The results are summarized in Figure 2. As can be qualitatively observed from Figure 1, the Cu(I) compounds all exhibit a low energy peak maximum in the region between 8983 and 8986 eV, which is plotted as a point in Figure 2 at the appropriate energy and normalized intensity. Alternatively, the Cu(II) compounds exhibit only a broad low-energy tail in the region below 8985.0 eV. The amplitude of these tails in the 8983–8985-eV region fall into two different groups, one including 34 normal Cu(II) complexes and the other for 6 covalent Cu(II) complexes (see Results, section A2). For each of the two groups, the extremes of the amplitude of the tails are plotted in Figure 2, these indicating the ranges that encompass all of the complexes in each group. For all 40 compounds studied, no Cu(II) model has a pre-edge maximum below 8985.0 eV and the intensity of the absorption tail over this spectral region is always significantly lower than the intensity of the peak of any of the Cu(I) complexes. Therefore, the appearance of a pre-edge peak below 8985.0 eV in the Cu absorption edge spectrum indicates the presence of Cu(I) in the sample. Alternatively, some Cu(I) complexes have their pre-edge intensity maxima at energies somewhat higher than 8985.0 eV (I-16, I-17, I-18). Therefore, the lack of a pre-edge feature below 8985.0 eV does not necessarily mean that Cu(I) is not present in the sample. A more systematic and quantitative analysis of these model edge results is given below.

(1) Copper(I) Complexes. As observed in Figure 2, the Cu(I) complexes exhibit a wide range in pre-edge peak energies and intensities that can be reasonably correlated with coordination number and analyzed within the context of a simple electronic structural description. From Figures 2 and 3a, the Cu(I) compounds with linear 2-coordinate structures (I-1, I-2, I-3, I-4, I-5) exhibit a sharp pre-edge absorption peak in the 8984-eV region, which for all compounds studied have the highest intensity (normalized absorption amplitude of 1.08 ± 0.10).[32] Polarized single-crystal XAS have been reported for compounds I-2 and I-3 and show this peak to be purely x,y polarized.[33] This requires the assignment of this 8983–8984-eV peak as the $1s \rightarrow 4p_{x,y}$ electric dipole-allowed transition. The alternative possible assignment as the $1s \rightarrow 4s$ transition would necessarily exhibit some z polarization, as intensity would derive from either a low symmetry distortion from $D_{\infty h}$ (crystallographic site symmetry is $\bar{1}$) or from a vibronic coupling mechanism. We further note that a shake-up transition mechanism is not available for the d^{10} configuration (see Discussion).

As presented in Figure 4, qualitative ligand field considerations predict that the threefold degeneracy of the $4p_{x,y,z}$ in the free Cu(I) ion will be split by the ligand field. For the linear 2-coordinate Cu(I) complexes ($D_{\infty h}$), this would involve repulsive interaction along the z axis which raises the energy of the antibonding copper $4p_z$ molecular orbital relative to the $4p_{x,y}$ levels. In addition, covalent ligand overlap along the z axis will reduce the intensity of the $1s \rightarrow 4p_z$ transition, as this mixing lowers the Cu $4p_z$

Table II. Compounds Used in K Edge Studies

	compounds[a]	ligation	ref[b]
I-1	$[Cu(xypz]_2(BF_4)_2$	N_2	a
I-2	$[Cu_2(EDTB)](ClO_4)_2$	N_2	b
I-3	$Cu(TMP)_2BF_4$	N_2	c
I-4	$Cu(2\text{-MIm})_2BF_4$	N_2[c]	c
I-5	$Cu(3,5\text{-DMP})_2BF_4$	N_2[c]	c
I-6	$[Cu(BBDHp)](BF_4)_{0.34}(PF_6)_{0.66}$	N_2 (+S_2 at 2.87 Å)	d
I-7	Cu_2O	O_2	e
I-8	$Cu(pze)BF_4$	N_2O	f
I-9	$[Cu(L_1\text{-pr})](BF_4)$	N_2S	g
I-10	$Cu_2ISOIM(t\text{-Bu})_2(pz)$	N_2O[c]	h
I-11	$[Cu_2(mxyN_6)](BF_4)_2$	N_3	i
I-12	$Cu(pza)BF_4$	N_3[c]	f
I-13	$[Cu(etu)_3]_2SO_4$	S_3	j
I-14	$[(C_6H_5)_4P]_2[Cu(SC_6H_5)_3]$	S_3	k
I-15	$[(C_6H_5)_4P]_2[Cu_4(SC_6H_5)_6]$	S_3	l
I-16	$[Cu(py)_4]ClO_4$	N_4	m
I-17	$Cu(tepa)BPh_4$	N_4	n
I-18	$[Cu_2(XYL\text{-}O\text{-})]PF_6$	N_3O	o
I-19	$Cu(2,5\text{-DTH})_2ClO_4$	S_4	p
II-1	$Cu(ImH)_4(ClO_4)_2$	N_4O_2	q
II-2	$Cu(ImH)_4SO_4$	N_4O_2	r
II-3	$Cu(ImH)_3(NO_3)_2$	N_4O_2	s
II-4	$Cu(NH_3)_4SO_4\cdot H_2O$	N_4O_2	t
II-5	$Cu_2(fsa)en\cdot CH_3OH$	$N_2O_2 + O_4$	u
II-6	$CuFe(fsaen)Cl\cdot 2.5H_2O$	N_2O_2	v
II-7	$Cu[(prp)_2en]Co(hfa)_2$	N_2O_2	w
II-8	$Cu[(prp)_2en]Cu(hfa)_2$	$N_2O_2 + O_6$	w
II-9	$Cu[(acp)_2en]CoCl_2$	N_2O_2	x
II-10	$Cu[(acp)_2en]CuCl_2$	$N_2O_2 + Cl_2O_2$	x
II-11	Cu citrate dihydrate	O_4O	y
II-12	Cu carnosine	N_2O_2N	z
II-13	$CuSO_4\cdot 5H_2O$	O_4O_2	aa
II-14	$Cu(acac)_2$	O_4	bb
II-15	anhydrous $Cu(formate)_2$	O_4O	cc
II-16	$Cu(OAc)_2\cdot H_2O$	O_5Cu	dd
II-17	anhydrous $Cu(propionate)_2$	O_5Cu	ee
II-18	Cu succinate dihydrate	O_5Cu	ff
II-19	CuO	O_4O_2	gg
II-20	$[Cu_2(L_8\text{-Et})(N_3)](BF_4)_2$	N_4O	hh
II-21	$[Cu_2(L_8\text{-Et})(OAc)](ClO_4)_2$	N_3O_2	hh
II-22	$[Cu(L_3)(H_2O)(OClO_3)](ClO_4)$	N_2O_2S	ii
II-23	$[Cu_2(L_8\text{-Et})(HCOO)](ClO_4)_2$	N_3O_2[c]	hh
II-24	$[Cu_2(L_8\text{-Et})(NCS)]\cdot(ClO_4)_2\cdot H_2O$	$N_4O + N_3OS$[c]	hh
II-25	$[Cu_2(L_8\text{-Et})(NO_2)](ClO_4)_2$	N_3O_2	jj
II-26	$[Cu_2(L_8\text{-Et})(pyrazolate)](ClO_4)_2$	N_4O[c]	hh
II-27	$[Cu_2(OH)(ClO_4)\supset A](ClO_4)_2\cdot CHCl_3$	N_3O_2	kk
II-28	$[Cu(pip)]_2(im)(NO_3)_3\cdot 2.5H_2O$	N_4O_2	ll
II-29	$[Cu(pmdt)]_2(2\text{-Meim})(ClO_4)_3$	N_4	ll
II-30	$[Cu(pmdt)]_2(Bzim)(ClO_4)_3\cdot H_2O$	$N_4 + N_4O$	ll
II-31	$[Creatinium]_2[CuCl_4]$	Cl_4	mm
II-32	$Cs_2[CuCl_4]$	Cl_4	nn
II-33	$Cu(phen)_2Cl_2\cdot 3H_2O$	N_4[d]	oo
II-34	$Cu(cyclam)(SC_6F_5)_2$	N_4S_2	pp
II-35	$Cu(14\text{-ane-}S_4)(ClO_4)_2$	S_4O_2	qq
II-36	$Cu[(C_2H_5)_2NCS_2]_2$	S_4SH	rr
II-37	$Cu(2,5\text{-DTH})_2(ClO_4)_2$	S_4	p
II-38	Cu[butyraldehyde-thiosemicarbazone]$_2$ green form	S_2N_2[c]	ss
II-39	Cu[butyraldehyde-thiosemicarbazone]$_2$ orange form	S_2N_2[c]	ss
II-40	Cu[2,3-butanedione-bis(thiosemicarbanonato)]	S_2N_2[c]	tt

[a] See the cited reference for the abbreviation of each compound. [b] Letters correspond to ref 31 in references and footnotes. [c] Structure not reported; however, the crystal structure of a copper complex with a similar ligand set has been solved. [d] Structure is not determined.

(32) The error limit is the actual range of values for all compounds of this type studied.

(33) Smith, T. A. G. Ph.D. Thesis, Stanford University, 1985.

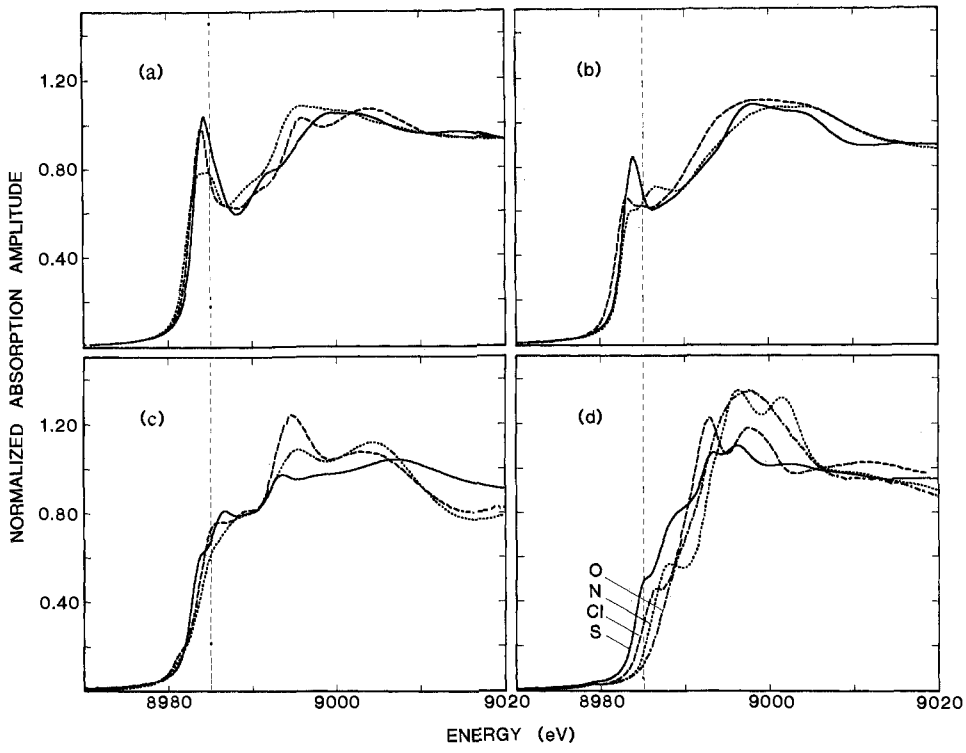

Figure 3. Normalized edge spectra (vertical dotted lines indicate 8985.0 eV): (a) 2-coordinate Cu(I) complexes I-1 (—), I-2 (- - -), and I-6 (···). Edge spectra of I-3, I-4, and I-5 are similar to those of I-1 and I-2 in the 8984-eV region as shown in Figure 2. (b) 3-coordinate Cu(I) complexes I-8 (—), I-10 (- - -), and I-11 (···). Edge spectra of I-9, I-12, I-13, I-14, and I-15 are similar to those of I-10 and I-11 in the 8984-eV region. (c) 4-coordinate Cu(I) complexes I-19 (—), I-16 (- - -), and I-17 (···). Edge spectrum of I-18 is similar to those of I-16 and I-17 in the 8986-eV region. (d) Tetragonal Cu(II) complexes with S_4 (II-37, —), Cl_4 (II-31, - - -), N_4 (II-1, ···), and O_4 (II-13, - · - ·) equatorial ligand sets. The amplitudes of the low energy absorption tails in the 8983–8985-eV region for the 34 normal Cu(II) complexes are similar to those of II-1, II-13, and II-31, and those for the 6 covalent Cu(II) complexes are similar to that of II-37.

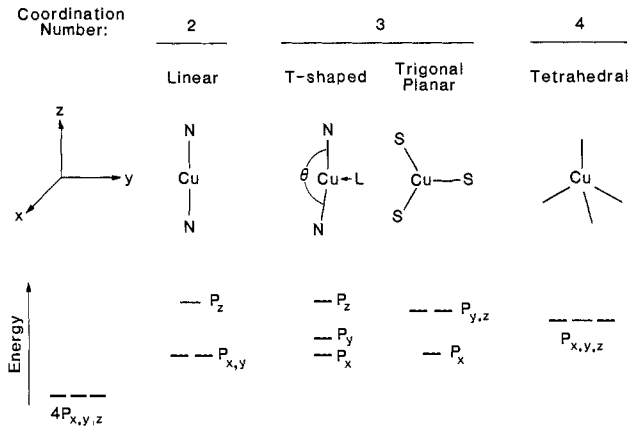

Figure 4. Ligand field splitting of copper 4p orbitals as a function of site geometry.

character in this antibonding orbital. Thus, the transition from 1s to the doubly degenerate $4p_{x,y}$ final state would result in an intense pre-edge peak at lower energy than the 1s → $4p_z$ transition. We note that while this description is generally in agreement with the experimental edge spectra for 2-coordinate complexes, compound I-6 (which is nominally 2 coordinate) has a broader, somewhat weaker pre-edge peak (Figure 3a). However, of the 2-coordinate complexes studied, only this complex has two additional sulfurs that are located 2.9 Å away in the x,y plane.[34] This S–Cu(I) distance should lead to some bonding interaction which will perturb the degeneracy of the $4p_{x,y}$ set and produce spectral changes as described below. Finally, it should be noted that unlike the other 2-coordinate complexes, Cu_2O (compound I-7) exhibits a pre-edge peak with lower intensity (normalized absorption amplitude of 0.64) which requires further study.

Three-coordinate Cu(I) complexes, with the one exception of I-8, have a normalized absorption amplitude of 0.63 ± 0.05 at 8984.0 eV (Figures 2 and 3b). Further, on the higher energy side of the main peak maximum (Figure 3b), there is often an additional feature which varies in energy position and intensity. The structures of these 3-coordinate compounds cover the range from T-shaped (I-9, I-10, I-11, and I-12 with a Cu–N bond length of ~1.90–1.92 Å and a N–Cu–N angle of ~160°) to trigonal planar (I-13, I-14, I-15 with a S–Cu–S angle of ~112–135°). Compound I-8, however, is closer to a linear two-coordinate structure with a Cu–N bond length of 1.87 Å and a N–Cu–N angle of 169°.[35] Compound I-8 exhibits a sharper pre-edge peak with higher intensity (normalized absorption amplitude of 0.84).

These observations are consistent with an extension of the above ligand field analysis where the 3-coordinate electronic structure is derived by perturbing the linear 2-coordinate system by including the effects of a third ligand (L) along the y axis and simultaneously decreasing the angle θ from 180° (Figure 4). The doubly degenerate $4p_{x,y}$ orbitals would now be expected to split, the p_y going to higher energy, and the 1s → $4p_y$ transition would decrease in intensity due to covalent mixing with the added ligand. The magnitude of both effects would be expected to increase as the extent of interaction with ligand L in Figure 4 increases. In the limit of a trigonal-planar structure (θ = 120°), p_y and p_z will be degenerate and to higher energy than the $4p_x$ level. Thus the 8984-eV peak would correspond to the 1s → $4p_x$ transition and is predicted to be polarized along the C_3 axis (which is the x axis in the coordination system in Figure 4).

Finally, in going from the 3-coordinate geometries to the 4-coordinate tetrahedral (T_d) structure, the $4p_{(x,y,z)}$ orbitals should be close to degenerate, but shifted to higher energy, and each 1s → $4p_i$ component transition would have reduced intensity.

(34) Schilstra, M. J.; Birker, P. J. M. W. L.; Verschoor, G. C.; Reedijk, J. *Inorg. Chem.* **1982**, *21*, 2637–2644.

(35) Sorrell, T. N.; Malachowski, M. R. *Inorg. Chem.* **1983**, *22*, 1883–1887.

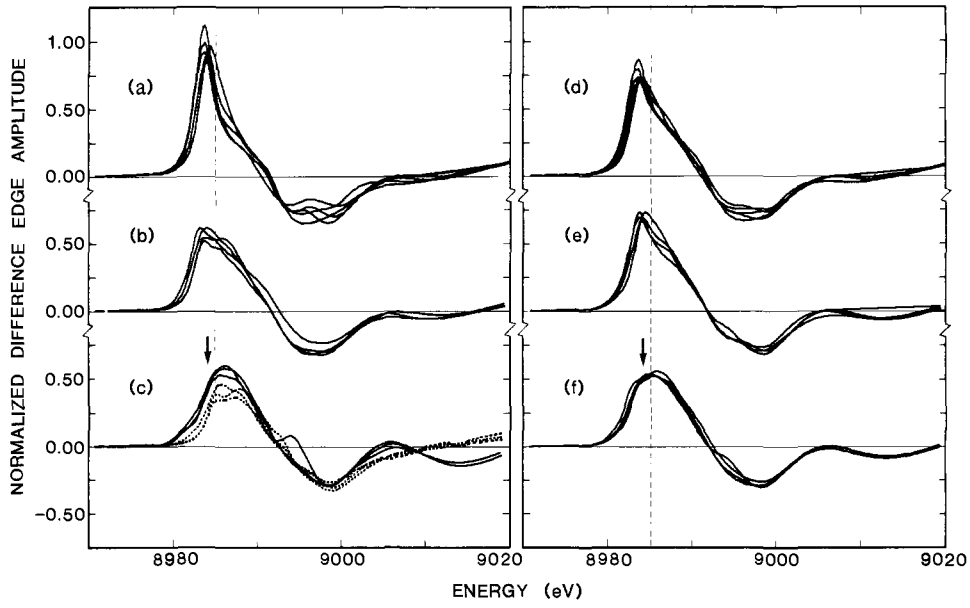

Figure 5. Representative normalized difference edge spectra for different coordination number Cu(I) and covalent Cu(II) complexes: (a) 2-coordinate Cu(I); (b) 3-coordinate Cu(I); (c) 4-coordinate Cu(I) (—) and covalent Cu(II) (···); (d) 2 + 3 coordinate; (e) 2 + 4 coordinate; (f) 3 + 4 coordinate binuclear Cu(I). Vertical lines indicate 8985.0 eV and the arrows in c and f indicate 8984 eV.

Compounds I-16, I-17, and I-18 (Figures 2 and 3c) show an edge peak that is at 8985.5 eV, ~1.5 eV higher in energy than the lowest energy peak maximum in the 2- and 3-coordinate complexes. The normalized absorption amplitude of these complexes is 0.72 ± 0.06. Two 4-coordinate complexes reported earlier,[13] $[Cu(HB(pz)_3)]_2$ and $CuCO(HB(pz)_3)$, also fit into this class. Finally, it should be noted from Figure 3c that unlike the other 4-coordinate complexes that all have N,O ligation, compound I-19 does exhibit a small peak at 8983.8 eV in addition to its main peak at 8986.6 eV. This low-energy feature appears to relate to the highly covalent S_4 ligand set of compound I-19, an observation that requires further spectroscopic study.

(2) Cu(II) Complexes. The K edges for a series of Cu(II) complexes which represent the range of observed spectra for the compounds in Table II are given in Figure 3d. All of the Cu(II) complexes studied have a very weak 8979-eV peak which corresponds to the 1s → 3d transition.[19] In addition, many Cu(II) complexes exhibit a rather intense peak (normalized absorption amplitude of 0.62–0.68) on the absorption edge at energies between 8986 and 8988 eV. The assignment of the 8986–8988-eV peak will be considered in the Discussion Section. In all 40 complexes studied, this Cu(II) peak is always observed at energies greater than 8985.0 eV and thus will not complicate the Cu(I) 1s → 4p region between 8983.0 and 8985.0 eV in Figure 2. Alternatively, all Cu(II) complexes do exhibit a pre-edge low-energy tail through this Cu(I) spectral region. As plotted in Figure 2, most of the Cu(II) complexes have a normalized absorption amplitude of 0.05–0.15 at 8984.0 eV. The six exceptions (II-35, II-36, II-37, II-38, II-39, and II-40) have higher absorption intensity in the 8983.0–8985.0-eV region (normalized height at 8984.0 eV = 0.24–0.38). From Figure 3d, this increase in the intensity of the low-energy tail is associated with the lower energy of the 8986-eV peak in these complexes. These exceptions have either S_4 or S_2N_2 equatorial ligation and are more covalent than the other Cu(II) complexes. Thus, their higher intensity appears to be related to this increased covalency, and in the following analysis, these six Cu(II) complexes are referred to as "covalent" Cu(II) complexes.

(3) Difference Edge Analysis. From the spectra presented above, it is possible to correlate Cu X-ray absorption pre-edge features with oxidation state and geometry. To further quantitate copper content we have calculated the normalized difference edge absorption spectra[23] by subtracting the normalized edge of a Cu(II) complex (averaged over the "non-covalent" model complexes) from that of a normalized edge of each of the Cu(I) and covalent Cu(II) complexes. This produces the characteristic derivative-shaped signal (inset Figure 1), and representative normalized difference edge spectra for the Cu(I) complexes are shown in Figure 5. Consistent with the edge data for each class of complexes given above, the difference spectra have a positive peak at 8983–8984 eV for 2- and 3-coordinate Cu(I) and at about 8986 eV for 4-coordinate Cu(I); a broad negative feature is observed for all complexes at 8990–9000 eV. Of particular importance for the quantitation are the amplitudes of these differences which have been averaged over all complexes of a given structural type and are summarized in Table III, with error limits reflecting the range of data for each set of complexes.

Table III. Normalized Difference Edge Energies and Amplitudes at Peak Maxima

CN	energy[a]	amplitude[a]	slope[b]
2	8983.6–84.2	0.99 ± 0.13	−0.20 to −0.45
3	8983.1–83.8	0.54 ± 0.08	0.0 to −0.06
4	8984.7–86.3	0.49 ± 0.,11	0.10 to 0.08
covalent Cu(II)	8985.8–88.0	0.42 ± 0.05	0.12 to 0.09
2 + 3	8983.6–84.2	0.75 ± 0.10	−0.07 to −0.11
2 + 4	8983.6–84.4	0.65 ± 0.07	−0.05 to −0.08
3 + 4	8983.7–85.8	0.48 ± 0.10	0.03 to 0.04
3 and 2 + 4	8983.1–84.4	0.59 ± 0.13	0.0 to −0.08
2 + 3 and 2 + 4	8983.6–84.4	0.71 ± 0.13	−0.05 to −0.11
1.5 [T2D − $^1/_3$ T1]	8983.6	0.58 ± 0.05	−0.06
T2D − (T2D + 60 × H_2O_2)[c]	8984.0	0.30 ± 0.03	

[a] At peak maxima. [b] The slope is defined as the best fit line extending between 8984 and 8986 eV of the spectrum and the unit is (normalized difference edge amplitude)/(eV). [c] Spectrum with convolved low resolution.

As the covalent Cu(II) compounds exhibit more intensity in the 8983–8985-eV region relative to the noncovalent Cu(II) complexes, and as it has been suggested that a very covalent Cu(II)[14] environment might have edge contributions similar to that of Cu(I), we have also calculated difference edges for the covalent Cu(II) complexes (Figure 5c). Although these difference edges look similar to those of 2- and 3-coordinate Cu(I) complexes, they have lower intensity at 8983–8984 eV and their maxima are broader and shifted to significantly higher energy. However, as can be seen in Figure 5c, it is not possible to distinguish 4-coordinate Cu(I) from covalent Cu(II) complexes based on their respective difference edge spectra.

In the next section, this difference edge analysis will be extended to quantitatively determine the extent of oxidation of the binuclear type 3 site in laccase. Thus, we have simulated the averaged difference edges for a binuclear Cu(I) system where each copper has a different coordination number (i.e., 2 + 3, 2 + 4, and 3 + 4). These normalized difference edges are shown in Figure 5d,e,f, and the averaged peak amplitudes are also included in Table III.

The energy and shape of the positive peaks in Figure 5 suggest that the edge spectrum can provide insight into the type of Cu present in the cuprous center of unknown coordination. In particular, only Cu(I) contributes a peak below 8985.0 eV; 2-coordinate Cu(I) leads to a sharper single peak, while 3, 2 + 3, and 2 + 4 all lead to a broader double-peaked feature in this region. Covalent copper(II), as well as 4 and 3 + 4 coordinate Cu(I), all lead to a broader higher energy feature that is easily distinguished from 2, 2 + 3, 3, and 2 + 4 coordinate Cu(I). In addition, 3 + 4 coordinate Cu(I) is different from 4 coordinate Cu(I) and covalent Cu(II) as it has a much larger relative amplitude at 8984 eV (see arrows in Figure 5, c and f). It is possible to further distinguish among these different structural possibilities based on the shape of the composite positive peak in Figure 5. The slope of this peak maximum can be defined as the best fit line extending from 8984 to 8986 eV. As given in Table III, the slope has a small positive value for 3 + 4 coordinate Cu(I) and then decreases in order over the series 3, 2 + 4, 2 + 3, and 2 coordinate Cu(I). On the basis of the ranges in slope obtained for the series of model complexes studied for each coordination number, there is only ambiguity in distinguishing between 3 and 2 + 4 or 2 + 4 and 2 + 3 coordinate copper(I).

Once the coordination number of copper is determined, the normalized difference edge intensities in Table III allow quantitation of the amount of cuprous ion present. The precision of the difference edge analysis depends on both the noise level of the data (normally very small) and the errors introduced by the normalization (±5%).[36] The accuracy depends on the extent to which the normalized difference edge amplitude for unity concentration is known. Ideally, fully oxidized and fully reduced forms of the complex of interest provide the highest accuracy. However, once the geometry of an unknown Cu sample is estimated from the shape of its difference edge spectrum, reasonable limits on the accuracy of the quantitation are still achievable. For 2-coordinate Cu(I) complexes, use of a peak height of 0.99 from Table III is accurate to ~13%, while for a 3 + 4 coordinate site, an amplitude of 0.48 can be used with ~20% error. On the basis of the ambiguity in distinguishing between 3 and 2 + 4 (or 2 + 4 and 2 + 3) coordinate Cu(I), a peak height averaged over these two geometries of 0.59 ± 0.13 (0.71 ± 0.13 for 2 + 4 and 2 + 3) should be used for quantitation.

(B) Redox Reactions of T2D Laccase. In order to accurately estimate the edge spectrum of the type 3 site in T2D laccase, it is necessary to remove the contribution from the type 1 copper. As the oxidized type 1 site is quite covalent,[37] its edge spectrum is similar to that of the covalent Cu(II) models in having higher intensity in the 8983–8985-eV region. The normalized edge of the oxidized blue copper in plastocyanin[38] is a reasonable model[39] for the type 1 site in T2D laccase and can be used to estimate its contribution to the T2D laccase edge spectrum. As the edge spectrum of T2D laccase contains contributions from three copper centers, one-third of the plastocyanin edge spectrum is subtracted from the edge spectra of both untreated and peroxide-treated laccase and the resultant spectra are then renormalized (×1.5). The difference edge spectra of these T1 subtracted T2D laccase spectra relative to the averaged noncovalent Cu(II) model compound edge are shown in Figure 6 and qualitatively confirm the presence of Cu(I) in the type 3 site of untreated T2D and the absence of Cu(I) in the peroxide-oxidized T2D.[40] The shape of

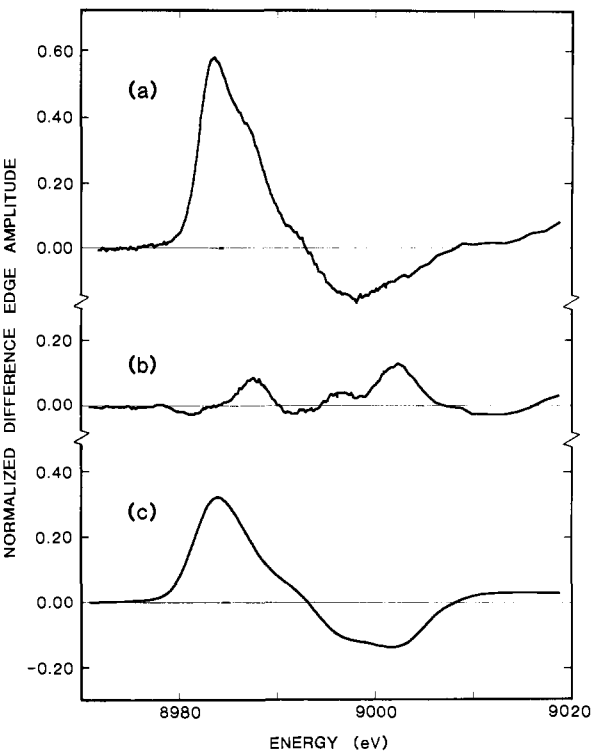

Figure 6. Normalized difference edge spectra of the type 3 site in T2D laccase derivatives. The edge spectrum of plastocyanin has been used to model the contribution of the type 1 (T1) Cu(II) in T2D. (a) $^3/_2$[T2D − $^1/_3$ T1 Cu(II)] − model Cu(II) (II-21); (b) $^3/_2$[(T2D + 60 × H_2O_2) − $^1/_3$ T1 Cu(II)] − model Cu(II) (II-21); and (c) convolved T2D − (T2D + 60 × H_2O_2).

the type 3 untreated T2D difference edge spectrum (Figure 6a, slope is −0.06 normalized difference edge amplitude/eV) is very similar to that of the 3 and 2 + 4 coordinate Cu(I) model complex spectra shown in Figure 5, spectra b and e. With use of the averaged difference edge intensity value for 3 and 2 + 4 coordinate Cu(I) model complexes (Table III), the normalized type 3 T2D difference edge amplitude (0.58) corresponds to 98 ± 22% Cu(I), while that of the type 3 in T2D reacted with 60-fold peroxide corresponds to 0 ± 8% Cu(I). This confirms our earlier qualitative observation[9] that the type 3 site in the T2D laccase is reduced and further indicates that the cuprous ions of this binuclear site are either both 3 or 2 + 4 coordinate.

For some metalloproteins, it has been observed[42] that X-irradiation can cause reduction of the metal sites during the course of the XAS measurements. Since the edge spectra reported here were measured in relatively short periods of time it is unlikely that photoreduction would be a problem. The integrated flux for all samples was less than 0.1 photon/Cu. Nevertheless, as described in the Experimental Section, we utilized both EPR and UV–vis absorption spectra to check for radiation-induced changes in the samples. For all of the samples the UV–vis spectra before and after irradiation were identical. For a few samples, measured with a wiggler beam line under dedicated conditions, we observed a small $g = 2.0$ radical signal in the EPR spectra after X-irradiation. However, in no case did we observe any change in the Cu(II) EPR signal, indicating that the X-ray induced radicals did not affect the Cu sites so long as the samples were kept frozen. Thawing and refreezing the samples gave EPR spectra identical with those before X-irradiation. As a further check for the possibility of X-ray induced changes in the Cu sites, we calculated the difference between the first and last X-ray absorption spectra which were recorded for each sample. In no case was there a Cu(I) minus

(36) From our experience, the variation in the amplitude of pre-edge features after normalization, using different polynomials and/or energy regions for the EXAFS region, is about 5%.

(37) (a) Colman, P. J.; Freeman, H. C.; Guss, J. M.; Murata, M.; Norris, V. A.; Ramshaw, J. A. M.; Venkatappa, M. P. *Nature (London)* **1978**, *272*, 319–324. (b) Adman, E. T.; Jensen, L. H. *Isr. J. Chem.* **1981**, *21*, 8–12. (c) Penfield, K. W.; Gewirth, A. A.; Solomon, E. I. *J. Am. Chem. Soc.* **1985**, *107*, 4519–4529.

(38) Tullius, T. D. Ph.D. Thesis, Stanford University, 1979.

(39) Spira, D. J.; Co, M. S.; Solomon, E. I.; Hodgson, K. O. *Biochem. Biophys. Res. Commun.* **1983**, *112*, 746–753.

(40) It should be noted that a Cu(II) edge estimated from the "noncovalent" Cu(II) models is appropriate for the T2D difference, as EXAFS studies have shown that no sulfur is coordinated to the type 3 site in laccase.[39,41]

(41) Woolery, G. L.; Powers, L.; Peisach, J.; Spiro, T. G. *Biochemistry* **1984**, *23*, 3428–3434.

(42) Chance, B.; Angiolillo, P.; Yang, E. K.; Powers, L. *FEBS Lett.* **1980**, *12*, 178–182.

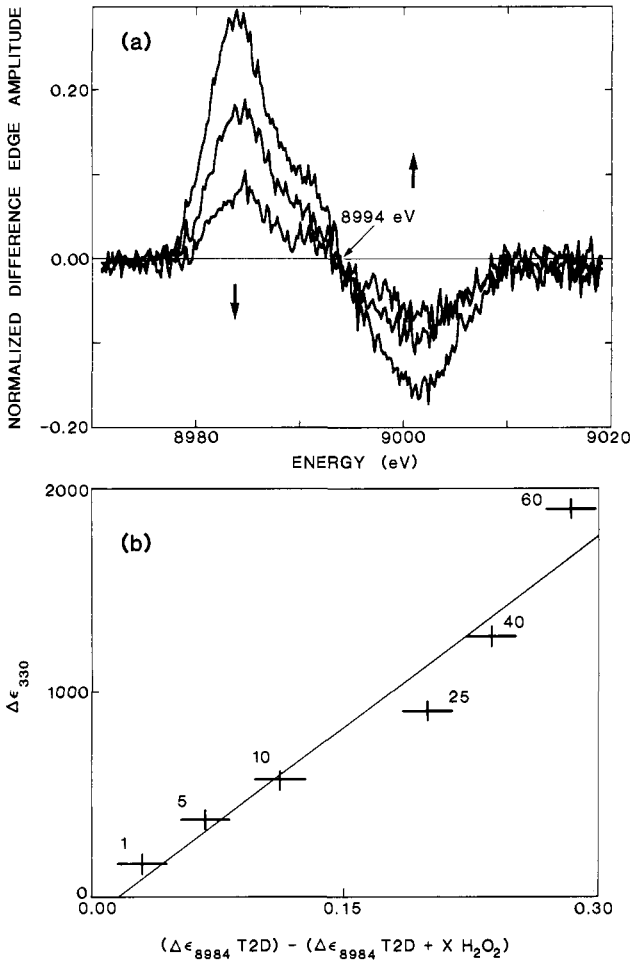

Figure 7. (a) Normalized difference edge spectra of T2D treated with 0, 10, and 25 protein equivalents of H_2O_2 relative to T2D + 60 × H_2O_2. Arrows indicate the direction of change on treatment with H_2O_2. (b) Correlation of $\Delta\epsilon_{8984}$ and $\Delta\epsilon_{330}$ for T2D laccase samples reacted with H_2O_2. All absorbance changes are referenced to the fully oxidized (60 × H_2O_2) sample. The stoichiometric excess of $[H_2O_2]$ is indicated for each data point (+).

Cu(II) difference signal above the noise level of the data, and from the signal/noise ratio we estimate that a change in Cu(I) of greater than 5% would have been detectable.

All the data analysis discussed thus far has used highest resolution data for model compound studies and for determination of Cu(I) content in T2D and peroxide-treated T2D protein. In the results described below, due to differences in resolution of the different data sets, we have convolved all of the data to low resolution before making quantitative comparisons (see Experimental Section).

Normalized difference edge analyses have been performed on six T2D samples prepared by similar methods from different isolations of native laccase. In all cases, difference spectra similar to those in Figure 6, a and b, are observed, the maximum variations in amplitude at 8984.0 eV being 10%. The consistency of these spectra indicates that the T2D + 60 × H_2O_2 edge spectrum can be used as the Cu(II) reference spectrum for calculating T2D difference edge spectra and that the normalized difference amplitude of 0.30 ± 0.03 for [T2D − (T2D + 60 × H_2O_2)] in Figure 6c and Table III can be used as the calibration standard for unity reduction of the type 3 site.[43] Since the major source of uncertainty in the difference methods arises from the determination of this amplitude factor, and since the protein type 3 site itself is the best model to use for studies of the binuclear copper center

(43) The amplitude in Figure 6c can be related to that in Figure 6a by multiplying by 3/2 to account for T1 copper and dividing by 0.84 to account for the low resolution condition used in Figure 6c.

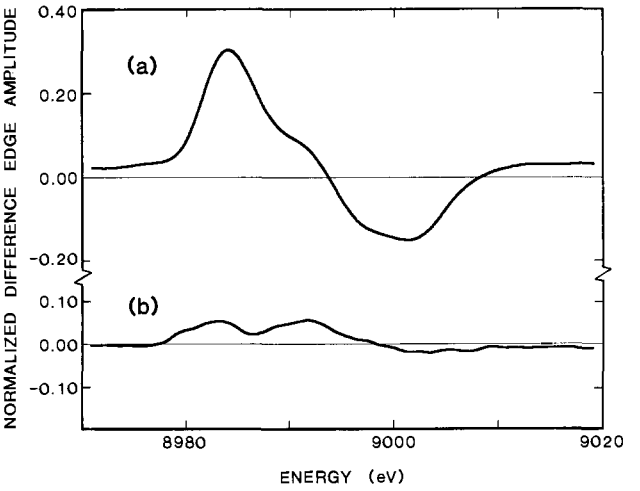

Figure 8. Normalized difference edge spectra for (a) (T2D + 25 × ferricyanide) − (T2D + 60 × H_2O_2) and (b) T2D − (T2D + 25 × ferricyanide). Spectra presented include effects of convolution with broadening function.

in laccase, this approach will significantly enhance the accuracy of the type 3 Cu(I) determinations and is used in all further oxidation state calculations of laccase.

While the above XAS edge studies of T2D laccase clearly demonstrate that peroxide is an oxidant for the reduced type 3 site in T2D laccase, it was not clear from these studies whether peroxide was also a ligand at the oxidized type 3 site. The $\Delta\epsilon_{330}$ ~ 2000 M^{-1} cm^{-1} which results from peroxide oxidation of the type 3 site could be due not only to endogenous ligand → Cu(II) CT intensity present in the type 3–oxidized T2D but also to O_2^{2-} → Cu(II) CT transitions of a peroxide bound complex of the oxidized T2D laccase. In order to further investigate the nature of this increase in 330-nm absorption intensity, we monitored the corresponding XAS difference edge and UV–visible absorption spectra for a series of T2D laccase samples reacted with 0, 1, 5, 10, 25, 40, and 60 protein equivalents of hydrogen peroxide. The dependence of the XAS difference edge structure on addition of 0, 10, and 25 × H_2O_2 is shown in Figure 7a. The isosbestic point at 8994 eV indicates that treatment with peroxide causes changes in only two absorbing species. Since there is no detectable change in the oxidation state of the type 1 copper by EPR, the difference edges must reflect changes only at the type 3 site. The decrease in difference edge amplitude is plotted vs. the appearance of the 330-nm absorption band with H_2O_2 addition in Figure 7b. Within experimental error, the increase in intensity of the absorption band at 330 nm correlates linearly to the decrease in the X-ray absorption feature at 8984 eV. Reaction with 60 × H_2O_2 yields an overall $\Delta\epsilon_{330}$ = 2000 M^{-1} cm^{-1} and 98 ± 22% change in type 3 binuclear Cu(I) to Cu(II); higher concentrations of H_2O_2 lead to irreversible protein damage. The linear correlation of these changes strongly indicates that H_2O_2 is acting as an oxidant throughout the titration. We note that these data would not exclude the possibility of peroxide binding to the binuclear cupric site with very high affinity ($K \geq 10^6$ M^{-1}) concomitant to oxidation of the cuprous centers. However, the intense absorption features observed for O_2^{2-} → Cu(II) CT transitions in oxyhemocyanin ($\Delta\epsilon_{345}$ ~ 20 000 M^{-1} cm^{-1}),[1,44] oxytyrosinase ($\Delta\epsilon_{345}$ ~ 14 000 M^{-1} cm^{-1}),[1,45] and peroxide Cu(II) model complexes ($\Delta\epsilon_{505}$ ~ 6300 M^{-1} cm^{-1}) for $[Cu_2(XYL\text{–}O\text{–})O_2]^{+2}$ [46a] and $\Delta\epsilon_{360}$ ~ 16,700 M^{-1} cm^{-1} for $[Cu_2(N4PY2)(O_2)^{+2}]$ [46b] suggest that an analogously intense transition should be observed for a peroxide bound complex of T2D laccase and such a feature is not present.

(44) Eickman, N. C.; Himmelwright, R. S.; Solomon, E. I. *Proc. Natl. Acad. Sci. U.S.A.* **1979**, *76*, 2094–2098.

(45) Himmelwright, R. S.; Eickman, N. C.; LuBien, C. D.; Lerch, K.; Solomon, E. I. *J. Am. Chem. Soc.* **1980**, *102*, 7339–7344.

(46) (a) Karlin, K. D.; Cruse, R. W.; Gultneh, Y.; Hayes, J. C.; Zubieta, J. *J. Am. Chem. Soc.* **1984**, *106*, 3372–3374. (b) Karlin, K. D.; Haka, M. S.; Cruse, R. W.; Gultneh, Y. *J. Am. Chem. Soc.* **1985**, *107*, 5828–5829.

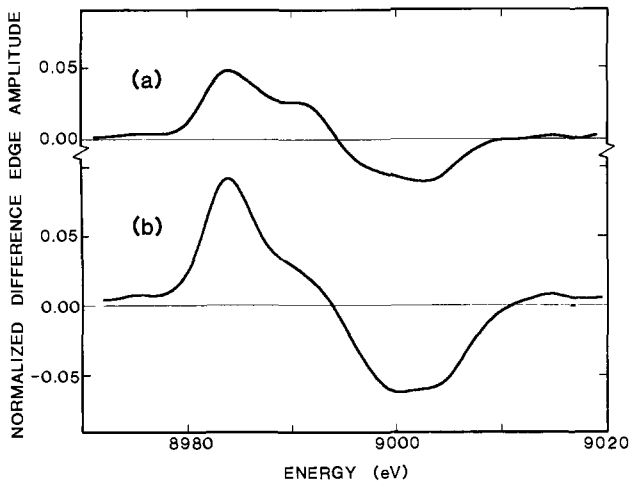

Figure 9. Normalized difference edge spectra for native laccase and its reactions with H_2O_2 and N_3^-. (a) Native laccase − (native laccase + 30 × H_2O_2); and (b) native laccase + 2.5 × N_3^-, 30 × H_2O_2) − (native laccase + 30 × H_2O_2). Spectra presented include effects of convolution with broadening function.

Finally, we have investigated the spectral changes associated with ferricyanide reactivity of T2D laccase. It has been suggested[11a] that ferricyanide can be used to fully oxidize T2D laccase. However, difference edge analysis (Figure 8a) of the reaction of 25 × ferricyanide with T2D gives a peak height of 0.30 which indicates that 100 ± 10% type 3 binuclear Cu(I) remains in the reacted enzyme. In particular, the difference spectrum between untreated and ferricyanide-treated T2D (Figure 8b) does not show the characteristic feature as in Figure 6c, indicating that there has been no significant change in the Cu(I):Cu(II) composition of the protein. Thus, under these conditions the binuclear cuprous site in T2D laccase is inert to ferricyanide oxidation.

(C) Peroxide Reactions of Native Laccase. The presence of binuclear cuprous sites in T2D laccase and their stability to oxidation by O_2 but not H_2O_2 suggested that the similar, although weaker, optical changes ($\Delta\epsilon_{325}$ = 800 M^{-1} cm^{-1}) observed in the peroxide reaction of the native enzyme,[6] originally interpreted as indicating peroxide binding to form a peroxy laccase derivative, might be due to oxidation. The normalized difference edge of native laccase minus native laccase reacted with 30 protein equivalents of peroxide at pH 6.0 is shown in Figure 9a. As EPR and optical spectra demonstrate that the type 1 and type 2 copper sites are not further oxidized,[47] the difference edge amplitude of 0.05 must again reflect a change at only the type 3 site. Calibrating to the fully reduced type 3 site in the untreated T2D laccase and allowing for the additional type 2 Cu(II) absorber present in native laccase, this corresponds to reduction of 22 ± 3% of the type 3 sites in the native laccase, as isolated. This reduction has also been suggested from azide binding studies.[48]

With use of the linear relationship between $\Delta\epsilon_{330}$ and $\Delta\epsilon_{8984}$ in T2D (Figure 7b), peroxide oxidation of reduced type 3 sites results in endogenous ligand → Cu(II) transitions which increase 330-nm intensity in native laccase by at least 440 ± 100 M^{-1} cm^{-1}. This calculation depends only on the relative values and is independent of the precise extent of type 3 reduction in T2D laccase. Previous studies[6] have used the $\Delta\epsilon_{325}$ = 800 M^{-1} cm^{-1} absorption and $\Delta(\Delta\epsilon)_{320}$ = −3.15 M^{-1} cm^{-1} CD features to conclude that peroxide binds to native laccase. If O_2^{2-} does bind to native laccase, the O_2^{2-} → Cu(II) CT transition at 325 nm must have ϵ < 360 M^{-1} cm^{-1}; on the basis of the intensity of these transitions in the hemocyanins, tyrosinase, and Cu(II) peroxide model complexes (vide supra), this limited increase in ϵ_{330} for native laccase cannot reasonably reflect peroxide → Cu(II) CT. The observation of

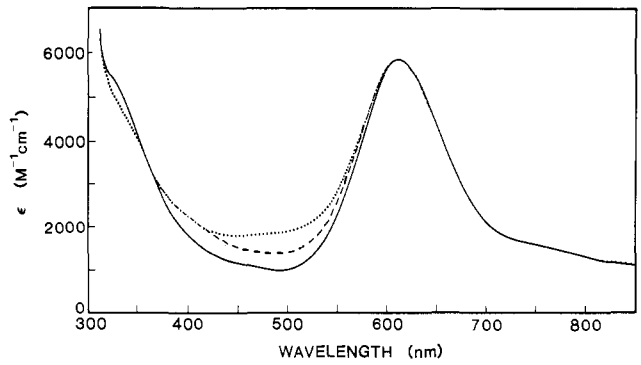

Figure 10. Electronic absorption spectra for native laccase (—), native laccase + 10 × N_3^- (- - -), and native laccase + 10 × N_3^-, 30 × H_2O_2 (···). Protein concentration is 0.15 mM, 1 cm path length.

22% reduced type 3 copper in native laccase indicates that the ϵ_{330} = 2800 M^{-1} cm^{-1} calculated from reduction studies[5] underestimates the ϵ_{330} for the fully oxidized native enzyme. Thus, a more appropriate value for the fully oxidized native laccase is ϵ_{330} = 3600 M^{-1} cm^{-1}.

In the presence of peroxide, low concentrations of azide (less than 10 protein equivalents) produce a charge-transfer spectrum very different from that observed when N_3^- is added to native laccase (Figure 10). While the native enzyme with 10 × N_3^- exhibits N_3^- → Cu(II) CT transitions at 500 and 410 nm with $\Delta\epsilon_{500}$ = 500 M^{-1} cm^{-1} and $\Delta\epsilon_{410}$ = 630 M^{-1} cm^{-1}, the native enzyme reacted with N_3^- in the presence of H_2O_2 shows an intense band at 500 nm with $\Delta\epsilon \sim$ 1300 M^{-1} cm^{-1}. Original studies[7b] interpreted these unique features as being evidence of a ternary complex of laccase with peroxide and azide, as the peroxy laccase[6] form was presumed to be valid. Having now demonstrated, however, that peroxide oxidizes but does not bind to the laccase active site, it is important to re-evaluate the spectral changes in Figure 10.

The normalized X-ray absorption difference edge of (native + 30 × H_2O_2, 2.5 × N_3^-) − (native + 30 × H_2O_2) is shown in Figure 9b.[49] For the equilibrated H_2O_2/N_3^- sample, $\Delta\epsilon_{500}$ = 1020 M^{-1} cm^{-1}; optical (type 1) and EPR (type 1 and type 2) spectroscopies demonstrate that the type 1 and type 2 copper centers are >90% oxidized, and hence the amplitude of 0.09 in the difference spectrum must correspond to reduction of 40 ± 4% of the type 3 copper sites. We note that N_3^- addition to native laccase in the absence of peroxide results in no change in total copper ion oxidation state composition. Thus, whereas peroxide oxidizes the reduced type 3 copper in native laccase, in the presence of azide, significant type 3 reduction occurs. This difference in peroxide redox activity indicates the potential for the type 3 copper pair must increase when azide is bound at the active site, consistent with the large difference in the N_3^- equilibrium binding constants for the reduced ($K_{eq} > 10^5$ M^{-1}) and oxidized ($K_{eq} \sim 10^2$ M^{-1}) protein at 298 K.

Protein and model studies[50,51] indicate that 500 nm is an unusually low energy for an N_3^- → Cu(II) CT transition, yet a weaker feature is observed at the same energy for N_3^- bound to native laccase. From Figures 9 and 10, the intensity of the N_3^- → Cu(II) CT feature at 500 nm appears to correlate with the fraction of binuclear cuprous type 3 sites in native laccase. (For complete type 3 reduction, $\Delta\epsilon_{500} \sim$ 2700 M^{-1} cm^{-1}.) Thus, the direct XAS edge determination of reduced type 3 copper in native laccase together with these studies of N_3^- reactivity demonstrate that the absorption feature at ~500 nm is associated with N_3^- binding to laccase molecules containing reduced type 3 sites, as

(47) We note that recent preparations of native laccase from 1984–1985 acetone powder have been found to contain up to 10% reduced type 2 copper, which is, however, less than 2.5% of the total laccase copper.

(48) Morpurgo, L.; Desideri, A.; Rotilio, G. *Biochem. J.* **1982**, *207*, 625–627.

(49) A lower concentration of N_3^- was used for the XAS experiments than in the optical spectrum of Figure 10, consistent with the higher protein concentration in the former study.

(50) Solomon, E. I.; Penfield, K .P.; Wilcox, D. E. *Struct. Bonding (Berlin)* **1982**, *53*, 1–57.

(51) Pate, J. E.; Karlin, K. D.; Reed, C. A.; Sorrell, T. N.; Solomon, E. I., manuscript in preparation.

was originally suggested by Morpurgo et al. from EPR studies[48,52] of N_3^- binding.

Discussion

From systematic studies on model complexes, it is possible to determine the presence of 2- and 3-coordinate Cu(I) from the low energy (~8984 eV) and peak shape of the X-ray absorption K edge of an unknown copper sample. Further, from the averaged, normalized, difference edge calculations over a series of model complexes (Table III), it is possible to quantitate the amount of 2- or 3-coordinate Cu(I) present. For a system of two copper ions where each copper can have a different coordination geometry (i.e., the type 3 site), it is still possible to recognize 2 and 3 + 4 coordinate Cu(I) and to quantitate these contributions; 3, 2 + 3, and 2 + 4 coordinate Cu(I) are quantitated with a somewhat lower accuracy due to the limited ambiguity in distinguishing among these possible coordination number mixtures. All the Cu(I) energy and intensity correlations are reasonably interpreted in terms of the ligand field splitting of the 4p orbitals as summarized in Figure 4.

As reported earlier,[14] it has been observed that covalent Cu(II) complexes exhibit more intensity in this 8983–8985-eV region. This increased intensity, however, is not found to complicate the difference edge analysis as no peak is present below 8985.0 eV. The intensity in the low-energy tail of the absorption results from the fact that the Cu(II) pre-edge peak (at energies ≥8986 eV, Figure 3d) occurs at somewhat lower energy relative to normal Cu(II) complexes. From Figure 3d, it is observed that there is, in fact, a systematic correlation of the decrease in the energy of the ~8986-eV absorption with the increase in covalency of the equatorial ligands. This spectral correlation is consistent with a shakedown assignment for this peak, involving a Cu 1s → 4p transition with simultaneous ligand-to-metal charge-transfer excitation.[22] A shakedown assignment is required in the interpretation of the Cu(II) 2p core XPS spectrum,[53] and its extention to the 1s core absorption appears appropriate and consistent with calculations.[22] Therefore, in addition to the features considered in the analysis of the 1s → 4p transition in Cu(I), the energy and intensity of this shakedown would also be dependent on the energy difference between the Cu(II) 3d and ligand valence orbitals, the extent of initial state covalency, and the final state orbital relaxation. A shakedown corresponds to a final state consisting of $(1s)^1...(3d)^{10}\underline{L}4p^1$ ($\underline{L}$ = ligand hole) which is at lower energy than the direct $(1s)^1...(3d)^9 4p^1$ transition. This would occur because of the greater effective nuclear charge felt by the Cu d electrons upon removing a 1s core electron. Thus, the energy of the shakedown should decrease as the ligand ionization energy decreases, which also increases covalency. We should also note that while no Cu(II) complex studied has a low-energy peak below 8985 eV, most of our reference complexes have a tetragonal geometry. This should not complicate the present analysis, however, as polarized single-crystal spectral studies on a tetragonal Cu(II) complex (II-3) have shown this peak to be z polarized and therefore a shakedown associated with the $4p_z$ transition.[21] Any geometric distortion of the tetragonal Cu(II) site will result in increased antibonding interaction along the long z axis and thus raise the energy of this level and the associated 1s → $4p_z$ transition.

Application of the XAS difference edge technique to T2D laccase demonstrates that in the absence of the type 2 copper, the type 3 site is 98 ± 22% reduced and that these cuprous ions are either both 3 coordinate or 2 + 4 coordinate. In native laccase, as isolated at pH 6.0, 22 ± 3% of the type 3 sites are reduced, and from low-temperature magnetic circular dichroism and absorption studies,[54] the extent of this reduction increases with decreasing pH. In the presence of N_3^- and O_2^{2-}, further reduction occurs and as much as 40% of the binuclear copper pairs can be stabilized in the reduced state. For all of the above chemical perturbations, the reduced type 3 site does not reoxidize in air. As shown in the previous paper,[2] the binuclear copper site in T2D laccase functions as two one-electron acceptors and does not bind exogenous ligands in a bridging mode. The lack of dioxygen reactivity therefore appears to be associated with both the relative thermodynamic difficulty of one-electron dioxygen reduction and the lack of exogenous ligand bridging which would stabilize the two-electron reduction. In native laccase, the type 3 coppers have the highest reduction potential[5] of the active site copper and thus should reduce first when a source of electrons is present. From the data presented herein, type 3 reoxidation by O_2 apparently does not readily occur when the type 1 and type 2 copper centers are already oxidized.

Peroxide increases the 330-nm intensity in T2D laccase and generates a feature qualitatively similar to that in the native enzyme. A related increase in the 330-nm region upon treatment of T2D with H_2O_2 has been assigned[11] as a O_2^{2-} → Cu(II) CT transition in analogy to earlier studies[6] of native laccase. However, the XAS edge peroxide titration and near-UV/vis correlation in Figure 7 demonstrate that the change in 330-nm intensity derives only from endogenous ligand → Cu(II) CT due to oxidation. Further, at least 55% of the change in 330-nm intensity for native laccase reacted with peroxide must also be due to oxidation, and the remaining $\Delta\epsilon_{330} \leq 360$ M^{-1} cm^{-1} is not reasonable spectral evidence for a peroxide-bound enzyme form. Thus at present, there is no evidence for a peroxide bound form of the type 3 site in laccase.

Finally we note that while the fully oxidized type 3 site in T2D displays a 330-nm feature similar to that in native laccase, there are quantitative differences in these features which are independent of contributions due to the type 2 Cu(II): T2D, $\Delta\epsilon_{330} = 2000 \pm 200$ M^{-1} cm^{-1}; native, $\Delta\epsilon_{330} = 3600 \pm 900$ M^{-1} cm^{-1}. These differences appear to relate to some structural difference in the T3 site on type 2 copper removal. As the 330-nm band in both T2D and native laccase can now be assigned as endogenous ligand → Cu(II) CT and EXAFS has determined that sulfur is not bound to the type 3 site in T2D laccase,[39,41] this band is probably associated with CT contributions from both N(his) and RO^- (where R can be either phenyl, H, or alkyl) ligands. Loss of an endogenous ligand or a change in overlap of the ligand with the Cu $d_{x^2-y^2}$ orbital could produce the intensity decrease in T2D relative to native. Alternatively, it has been observed in reduction studies of oxidized T2D (see previous paper) that this band is mostly eliminated by one electron equivalent indicating that a pair of Cu(II)'s is required for the intensity mechanism. Thus, a change in coupling between the coppers could also contribute to the intensity change. In either case, the perturbation of the type 3 site on the type 2 removal is not so great as to alter the basic structural feature of the site. In oxidized T2D, as in native laccase, the Type 3 cupric site remains EPR nondetectable, and hence, coupled by a superexchange pathway which is a protonatable bridging ligand with an intrinsic pK_a greater than 6.[2,54]

Acknowledgment. We acknowledge the National Institutes of Health (DK-31450 to E.I.S.) and the National Science Foundation (CHE-8512129 to K.O.H.) for support of this research. Synchrotron beam time was provided by the Stanford Synchrotron Radiation Laboratory, which is supported by the U.S. Department of Energy and the Division of Research Resources of the National Institutes of Health. Finally, we thank Professors Robert R. Gagne, Kenneth D. Karlin, Stephen J. Lippard, Christopher A. Reed, Jan Reedijk, and Thomas N. Sorrell for providing many of the Cu model complexes.

(52) We note that the 30 × H_2O_2, 2.5 × N_3^- protein sample displays a 77 K EPR signal very different from that of N_3^- bound to fully oxidized laccase but quite similar to that of the azide-bound native sample in the presence of reductant in ref 48.

(53) Gewirth, A. A.; Cohen, S. L.; Schugar, H. J.; Solomon, E. I. *Inorg. Chem.* **1987**, *26*, 1133–1146.

(54) (a) Allendorf, M. D.; Spira, D. J.; Solomon, E. I. *Proc. Natl. Acad. Sci. U.S.A.* **1985**, *82*, 3063–3067. (b) Spira-Solomon, D. J.; Allendorf, M. D.; Solomon, E. I. *J. Am. Chem. Soc.* **1986**, *108*, 5318–5328.